Journal of Applied Fluid Mechanics, Vol. 9, No. 6, pp. 2781-2790, 2016.
Available online at www.jafmonline.net, ISSN 1735-3572, EISSN 1735-3645.

Applying Different Strategies within OpenFOAM to Investigate the Effects of Breakup and Collision Model on the Spray and in-Cylinder Gas Mixture Attribute

P. Ghadimi†, M. Yousefifard and H. Nowruzi

Department of Marine Technology, Amirkabir University of Technology, Tehran

†*Corresponding Author Email: pghadimi@aut.ac.ir*

(Received January 31, 2016; accepted May 3, 2016)

ABSTRACT

In the current study, a 3-D numerical simulation of two-phase flow has been conducted in a direct injection CI engine using the Eularian-Lagrangian approach and a new breakup model. The newly modified breakup scheme has been implemented for simulating the ultra-high pressure diesel injection. The effects of droplet breakup and collision model on the spray and in-cylinder gas characteristics have been examined using the open source code OpenFOAM. Spray penetration and cone angle are investigated as spray properties and surrounding gas motion are studied by in-cylinder gas velocity and pressure distribution for non-evaporating conditions. In addition, vapor penetration of the evaporating spray is presented to study the effects of current scheme on the evaporating condition. The continuous field is described by RANS equations and dynamics of the dispersed droplet is modeled by Lagrangian tracking scheme. Results of the proposed modified KHRT model are compared against other default methods in OpenFOAM and favorable agreement is achieved. Robustness and accuracy of different breakup schemes and collision models are also verified using the published experimental data. It is demonstrated that the proposed breakup scheme and Nordin collision model display very accurate results in the case of ultra-high pressure injection.

Keywords: Diesel spray; Ultra-high pressure; Droplet breakup; Collision model; OpenFOAM.

1. INTRODUCTION

Increasing demand for low polluting and efficient diesel engines has lead to numerous studies related to different processes that take place in them. Study of diesel sprays is important for many applications in the field of CI engines. Performance of the diesel injection engines mainly depend on the spray characteristics. Spray behavior is affected by many parameters such as injector geometry, injection pressure and ambient properties. Accurate modeling of the spray breakup and droplet collision is the most important element of numerical modeling of the diesel sprays. Spray behavior including the atomization, breakup, and collision of droplets during injection process has included majority of the past research. In spite of the importance of atomization, the mechanisms of breakup and collision are still not well understood.

Recently, computational power improvements have led to advanced CFD codes and numerical methods that provide reliable results. Thus, using CFD code for solution of diesel spray can be considered the best remedy. Effects of injection and ambient parameters on the spray characteristics have been investigated through these numerical methods (Moreira *et al*., 2010).

There have been different numerical studies on primary and secondary atomization phenomena. Liquid spray breakup can be caused by Kelvin-Helmholtz (KH) and Rayleigh-Taylor (RT) instabilities at the interface of the two fluids. The KH instability is due to high shear at the interface, while the RT breakup theory is based on the stability of liquid-gas interfaces during the acceleration in normal direction to the plane. The most commonly used breakup models are based on KH and RT theories (Reitz and Bracco, 1982).

Som *et al*. (2010) investigated the influence of primary breakup model on the process of air-fuel mixture. They conducted 3-D simulations with detailed chemistry using a particular breakup

model. Hosseinpour *et al*. (2009) used a CFD code for investigating the effect of breakup model on the spray and the mixture formation in a heavy-duty diesel engine. Also, Turner *et al*. (2012) proposed a breakup model for analyzing the evolution of transient fuel sprays characterized by a coherent liquid core emerging from the injection nozzle, throughout the injection process. Wang *et al*. (2010) presented a detailed experimental inspection of the biodiesel spray characteristics for the high injection pressure up to 300 MPa. On the other hand, Zhu *et al*. (2014) reported a detailed experimental data of the free spray and spray characteristics of flat-wall impinging under ultra-high injection pressures.

Roisman *et al*. (2007) investigated the effect of ambient pressure on penetration of the diesel spray experimentally and theoretically. Penetration length and the cone angle of the spray were measured at various injection pressures and ambient pressures. Kamali and Mofarrahi (2012) numerically investigated the effects of spray breakup and droplet collision models on in-cylinder diesel spray. Shervani-tabar *et al*. (2013) carried out a numerical simulation for studying the effect of injection pressure on spray penetration length. In recent years, Gjesing *et al*. (2009), Kassem *et al*. (2011), Vourinen *et al*. (2011), Wehrfritz *et al*. (2013), Ghadimi and Nowruzi (2016) ,and Yousefifard *et al*. (2014a,b, 2015) have utilized open source codes as efficient methods for modeling the diesel spray. However, none of these studies have concentrated on high pressure diesel injection.

In the current paper, an Eulerian-Lagrangian approach has been utilized using different breakup and collision models in order to find the most acceptable model for ultra-high pressure diesel injection. Main attention of this study is focused on the prediction of the effect of advanced breakup model on spray and ambient gas characteristics. A new breakup model is developed to consider the transient condition of spray. Current study treats the direct injection of fuel at ultra-high pressures. Ignition is not simulated in this work. The computational tool used in this work is OpenFOAM software. Results of numerical simulations in this study have been compared against published experimental data reported by Zhu *et al*. (2012, 2014) in the cases of spray and gas characteristics.

First, governing equations in two-phase flow are presented and spray breakup and droplet collision models are discussed in more depth. Then, the advanced combined breakup model is presented. Subsequently, details of an experimental data which is used to validate the current model are presented. Later, the obtained results are compared against experiments. Finally, conclusion is presented in the last section.

2. GOVERNING EQUATION

Compressible flows can be expressed by the Navier-Stokes (NS) equations describing the conservation of mass and momentum. On the other hand, Lagrangian Particle Tracking (LPT) approach is usually employed for the simulation of dispersed phase.

2.1 Navier-Stokes Equations

In the current simulation, NS equations for the conservative variables of continuous field are as follows (Stiesch, 2003):

Equation of mass conservation is:

$$\frac{\partial \rho}{\partial t}+\frac{\partial}{\partial x_j}\left(\rho u_j\right)=\dot{S}_{evap} \tag{1}$$

Equation of momentum conservation is:

$$\frac{\partial \rho u_i}{\partial t}+\frac{\partial}{\partial x_j}\left(\rho u_j u_i-\tau_{ij}\right)=-\frac{\partial P}{\partial x_i}+\dot{S}_{i,mom} \tag{2}$$

where $u=\left(u_1,u_2,u_3\right)$ is the velocity vector, P is the pressure, ρ is the flow density, and τ_{ij} is the resolved stress tensor. $\dot{S}$ is the source term due to evaporation, momentum, and heat transfer. Pressure-velocity coupling has been carried out using PISO algorithm (Ferziger, 2002), and favre time averaging is applied to velocity components. Also, the standard $k-\varepsilon$ turbulence model (Jones and Launder, 1972) is utilized in RANS modeling scheme

2.2 Droplet Motion

Particles dynamics is described by Newton's equation of motion. It is assumed that drag force acting on a droplet leads to the equation of motion as in.

$$\frac{1}{6}\rho_p \pi d^3 \frac{du_p}{dt}=\frac{1}{2}\left(u_g-u_p\right)\left|u_g-u_p\right|\rho_g C_D \frac{\pi d^2}{4} \tag{3}$$

where u_p is the particle velocity, u_g is the gas velocity that is interpolated on the particle position from the adjacent cells and C_D is the droplet drag coefficient that can be defined by

$$C_D=\begin{cases}\dfrac{24}{\mathrm{Re}_p}\left(1+\dfrac{1}{6}\mathrm{Re}_p^{2/3}\right), & \mathrm{Re}_p<1000\\ 0.424, & \mathrm{Re}_p\geq 1000\end{cases} \tag{4}$$

The droplet Reynolds number is given by $\mathrm{Re}_p=\dfrac{\left|u_g-u_p\right|d}{\upsilon_g}$.

2.3 Droplet Breakup

Breakup modeling is the main sub-model in spray simulation. The spray atomization process can be divided into two main steps; primary and secondary breakup. In the primary breakup process, in-cylinder mixture formation has been provided. The task of primary breakup model is to determine the starting conditions such as initial diameter of the drops and spray angle. The most popular model of the primary breakup is Blob method that was

developed by Reitz and Diwakar (1987). Based on this model, the diameter of the injected blobs is equal to the nozzle diameter and number of drops injected per unit time is determined from the mass flow rate profile. As noted earlier, secondary breakup process is described by aerodynamic stripping of smaller droplets from the larger droplets (Kelvin-Helmholtz instability) or disintegration of larger droplets into smaller ones due to the effect of normal stresses (Rayleigh-Taylor instability). Breakup models that are mostly used in modeling of the diesel spray are described next.

2.3.1 Wave Breakup Model

WAVE breakup model was originally developed by Reitz (1987) and is based on the growth of KH instabilities on liquid surface at the interface of two phases that have different densities. Radius of the injected droplets, i.e. r_d, is assumed to continuously decrease during the breakup process, as in

$$\frac{dr_d}{dt} = -\frac{r_d - r_s}{\tau_{bu}} \tag{5}$$

where τ_{bu} is the characteristic breakup time of the droplet, and r_s is radius of stable droplets as in

$$r_s = \begin{cases} B_0\Lambda & B_0\Lambda \le r_d \\ \min\begin{pmatrix} (3\pi r_d^2 U_m / 2\Omega)^{0.33} \\ (3r_d^2\Lambda/4)^{0.33} \end{pmatrix} & B_0\Lambda > r_d \end{cases} \tag{6}$$

Here, $B_0 = 0.61$ is the model constant and Λ and Ω are the corresponding wave-length and growth rate of the fastest growing wave on the surface of the liquid jet.

$$\Omega_{KH} = \sqrt{\frac{\sigma}{\rho_l r_0^3}}.\frac{0.34 + 0.38We_g^{1.5}}{(1+Oh)(1+1.4Ta^{0.6})} \tag{7}$$

$$\Lambda_{KH} = 9.02r_0.\frac{(1+0.45\sqrt{Oh})(1+1.4Ta^{0.7})}{(1+0.865We_g^{1.67})^{0.6}} \tag{8}$$

where

$$Oh = \frac{\sqrt{We_l}}{\mathrm{Re}_l}, Ta = Oh\sqrt{We_g}, \quad We_g = \frac{\rho_g r_0 u_{rel}^2}{\sigma},$$

$$We_l = \frac{\rho_l r_0 u_{rel}^2}{\sigma}, \ \mathrm{Re}_l = \frac{\rho_l r_0 u_{rel}}{\mu_l}, \tag{9}$$

while r_0 is the droplet radius before the breakup, $u_{rel} = |u_d - u|$ is the relative velocity between the droplet and the surrounding gas, Oh is the Ohnesorge number, Ta is the Taylor number, We_g and We_l are the Weber numbers for the liquid and gas respectively and Re_l is the Reynolds number for the liquid.

Also, the breakup time is given by

$$\tau_{bu} = 3.7626\frac{B_1 R}{\Lambda\Omega} \tag{10}$$

where B_1 is an adjustable model constant which varies approximately between $\sqrt{3}$ and 60 (Reitz, 1987) depending on the injector type. A higher value of B_1 leads to reduced breakup and increased penetration, while a smaller value on the other hand, results in an increased spray disintegration, faster fuel-air mixing, and reduced penetration. Default value in the software is $B_1 = 40$ and some higher values up to 60 have been suggested.

2.3.2 TAB Breakup Model

O'Rourke and Amsden (1987) proposed the so-called Taylor analogy breakup (TAB) model that is based on Taylor analogy. In Taylor analogy model, it is assumed that droplet distortion can be described as a one-dimensional, forced, damped, harmonic oscillation, similar as in a spring-mass system. Standard TAB model has been modified to an Enhanced TAB called ETAB model which uses new strategy for describing the droplet breakup process (1997).

2.3.3 Pilch-Erdman Breakup Model

The Pilch-Erdman breakup model was derived for liquid drops at a higher velocity flow field which is less dense than the droplets (Pilch and Erdman, 1987). The mechanisms of acceleration-induced droplets breakup have been reviewed by Pilch and Erdman (1987) and a triangular relationship based on the concept of a critical Weber number, breakup time and velocity history data has been presented. Relations for the total breakup time have been presented by

$$T = 6(We-12)^{-0.25}, 12 \le We \le 18,$$

$$T = 2.45(We-12)^{-0.25}, 18 \le We \le 45, \tag{11}$$

$$T = 14.1(We-12)^{-0.25}, 45 \le We \le 351,$$

$$T = 0.766(We-12)^{-0.25}, 351 \le We \le 2670,$$

and

$$T = 5.5, 2670 \le We \tag{12}$$

In the current study, the default Pilch-Erdman model of OpenFOAM code has been used without any modifications.

2.3.4 KHRT Breakup Model

This hybrid model combines the effects of Kelvin-Helmholtz waves driven by aerodynamic forces with Rayleigh-Taylor instabilities due to acceleration of shed drops ejected into free stream conditions (Reitz, 1987). The Rayleigh-Taylor model is based on theoretical work of Taylor (1950). RT instabilities appear when acceleration is normal to the interface of two fluids of different

densities. Similar to KH instabilities, the wavelength and growth rate of the fastest growing wave can be obtained through linear stability analysis. Liquid viscosity and gravity are neglected, when performing these calculations.

$$\Omega_{RT} = \sqrt{\frac{2}{3\sqrt{3\sigma}} \frac{\left[a\left(\rho_l - \rho_g\right)\right]^{1.5}}{\rho_l - \rho_g}} \tag{13}$$

$$\Lambda_{RT} = C_3 2\pi \sqrt{\frac{3\sigma}{a\left(\rho_l - \rho_g\right)}} \tag{14}$$

Drops can only break if the wavelength (Λ_{RT}) is smaller than their diameter.

In the KHRT model, aerodynamic force on the drop flattens it into the shape of a liquid sheet, and the decelerating sheet breaks into large-scale fragments by means of RT instability. The KH waves with a much shorter wavelength originate at the edges of the fragments, and these waves break into micrometer-size drops, as shown in Fig.1. In this particular case, the default KHRT breakup model in OpenFOAM software has been used in its original form.

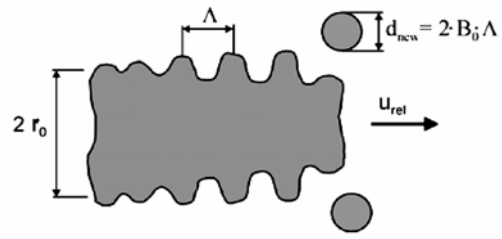

(a)

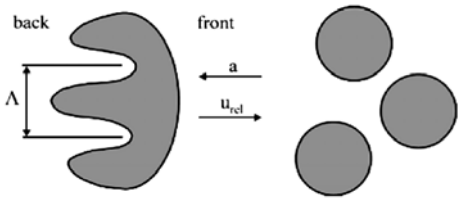

(b)

Fig. 1. Illustration of the Kelvin-Helmholtz Model (a) and Rayleigh-Taylor instability (b).

2.3.5 Advanced KHRT Breakup Model

The KHRT model is the most popular of all hybrid breakup models. It has been successfully validated against experimental data and used by many authors to predict the disintegration process of high-pressure diesel sprays (Baumgarten, 2006).

The proposed scheme for modeling the KH instability has been modified to incorporate the transient effects provided by Sazhin *et al*. (2008). Their modified WAVE breakup model introduced a new breakup time. In Eq. (10), the model constant was modified as

$$B_1^{\mathrm{mod}} = B_1\left(1 + C_1\left(a^+\right)^{C_2}\right) \tag{15}$$

where

$$a^+ = 2\sqrt{\mathrm{Re}_2}\,\frac{r_d}{U_{inj}^2}\frac{dU_{inj}}{dt} \tag{16}$$

is the acceleration parameter, C_1 and C_2 are adjustable model constants, and Re_2 is the gas Reynolds number. Based on the research presented by Turner *et al*. (2012), C_1 and C_2 have been set equal to 1 and 0.2, respectively.

In the current study, the modified breakup time model that was proposed by Sazhin *et al*. (2008) has been implemented and a new advanced KHRT breakup model is developed to simulate ultra-high pressure diesel injection. This modified model is added to the sprayFoam solver of the OpenFOAM 2.1.1 software.

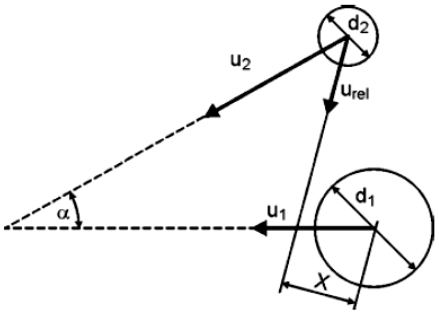

Fig. 2. Schematic of the geometric collision parameters.

2.4 Droplet Collision

In the current study, two different models have been used for simulation of the droplet collision. The O'Rourke collision model is based on calculation of collision probability for two droplets in the same cell.

O'Rourke collision model has been strongly grid dependent. There is a new collision model presented by Nordin (2001) that calculates the paths of all parcels and collides those that will intersect within the same time step. Therefore, a new algorithm has been defined for calculation of the parcels paths. This procedure reduces the computational load of the collision modeling. The probability for a collision is now given as

(17)

$$\left(\frac{\frac{1}{2}\left(d_1 + d_2\right)}{\max\left(\frac{1}{2}\left(d_1 + d_2\right), \left|X_{1,new}\left(t_\alpha\right) - X_{2,new}\left(t_\beta\right)\right|\right)}\right)^{C_{space}} e^{-\frac{c_{time}\left(t_\alpha - t_\beta\right)}{\Delta t}}$$

where $\left|X_{1,new}-X_{2,new}\right|$ is the smallest distance between two parcels during the time step, and C_{time} and C_{space} are model constants that control the collision rate in time and space, respectively. Fig. 2 presents geometric collision parameters. In the current paper, the above collision models are known as O'Rourk and trajectory model, respectively.

3. COMPUTATIONAL MODEL

A simple grading structured mesh is implemented for the numerical simulation of single hole injector under three particular sets of experimental conditions presented by Zhu *et al*. (2014) and Engine Combustion Network (ECN) is used in different simulations which were presented by Xue *et al*. (2014). OpenFOAM 2.1.1 is implemented in this study and simulation is accomplished in parallel using 16 processors. Grid sensitivity studies have been carried out for three different mesh sizes. Coarse mesh contains 0.5×10^6 cells for the current simulations. Number of the cells involved is 1.2×10^6 for the considered fine mesh. Droplet penetration as the main key parameter of the diesel spray is used as the basis of comparison and as a result, 1.0×10^6 cells are selected for this study.

A constant volume chamber of size (50×50×100 mm3) is used and according to grid independency study based on the spray penetration comparison at various time steps, 1.0×106 cells and 2,000,000 parcels are applied to this domain. Simulation domain and the considered mesh are illustrated in Fig. 3. Specifications and operating conditions of this model are listed in Table 1. Case 1 is related to the experimental conditions of Zhu *et al*. (2014). Cases 2 and 3 have been implemented based on the conditions named as spray A by the ECN Sandia.

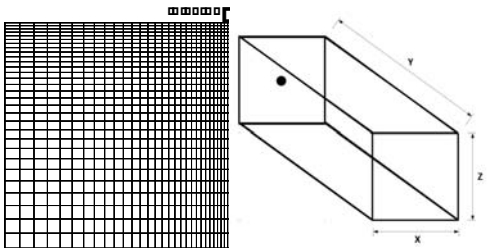

Fig. 3. Simulation domain and the considered mesh.

Figure 4 illustrates the fuel mass flow rate vs. time at 100, 200 and 300 MPa presented by Zhu *et al*. (2012).

4. RESULTS AND DISCUSSION

In order to examine the effect of breakup models on spray characteristics under ultra-high pressure conditions, the obtained results are compared against the published experimental measurements of Zhu *et al*. (2014) for non-evaporating and non-reacting sprays. These comparisons have been carried out in two fields; spray characteristics and in-cylinder flow properties. Also, evaporating spray characteristics have been examined using ECN Sandia condition and the resulting spray penetration has been compared with the available experimental data.

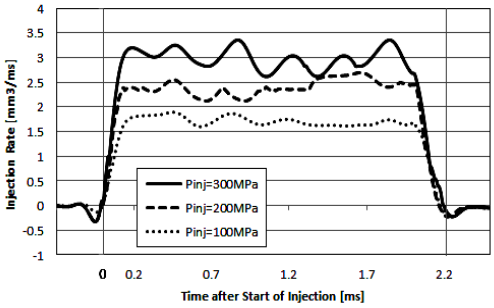

Fig. 4. Injector mass flow rate (Zhu *et al*., 2012).

Table 1 Simulation conditions

	Case 1	Case 2	Case 3
Injection duration (ms)	2.2	1.5	1.5
Density (g/m^3, 300K)	0.86	0.76	0.76
Surface tension (N/m, 300K)	0.025	0.025	0.025
Ambient gas temperature (K)	300	900	300
Nozzle Diameter (mm)	0.08	0.09	0.09
Injection pressure (MPa)	100, 200 and 300	150	150
Ambient gas	Nitrogen	Air	Nitrogen
Ambient gas density (kg/m^3)	15	22.8	22.8

4.1 Spray Characteristics

Figure 5 shows the spray form at the time t=1.0 ms for various break up models, compared against experimental shape. It is clear that Pilch-Erdman breakup model is unable to provide acceptable jet penetration and the corresponding spray shape does not match the experimental results. However, in the KHRT model, jet penetration and cone angle are both acceptable, as evidenced in Fig. 4. On the other hand, the modified KHRT model presents more acceptable spray shapes and penetration.

Figure 6 presents the simulated spray droplet cloud against time after the start of injection (ASOI) at P_{inj}=100MPa using the modified KHRT breakup model. It is quite evident that as time increase during the injection procedure leads to higher values of spray penetration.

Spray tip penetration, as a function of time, is perhaps the most common quantity to be studied in the field of diesel spray research, since the tip position can be easily detected from the spray shadowgraph images (Heywood, 1988). The predicted jet penetration lengths for all cases are

displayed and compared against experimental results in Fig.7. As observed in Fig.7, the numerical jet fuel penetration distance for the Pilch-Erdman, WAVE, KHRT, and modified KHRT breakup models agree in trend with the experimental data up until 2ms. However, the modified KHRT model which is introduced in this study and implemented in the OpenFOAM code shows almost exact similarity with the experimental data, especially at the beginning of injection process.

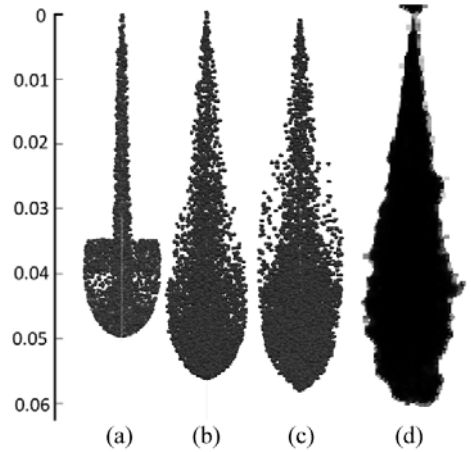

Fig. 5. Spray shapes for the Pilch-Erdman (a), KHRT (b) and Modified KHRT (c) breakup models and experiment result (d) at time t= 1.0 ms and P_{inj}=100MPa (Case 1).

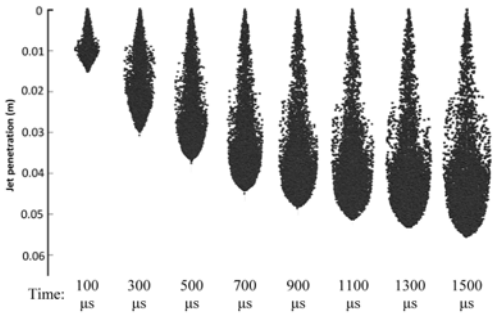

Fig. 6. Plot of spray shapes for modified KHRT breakup model up to t=1.5 ms (Case 1).

Indeed, modified KHRT model with mean square error (RMSE) of 0.0032 has the best accordance with the experiment. Also, KHRT breakup model with RMSE=0.0054 is shown to be next proper breakup model. On the other hand, Plich Erdman with RMSE=0.0077 displayes the least compliance with the experiment.

The effects of droplet collision model on the spray tip penetration have been presented in Fig. 8. As shown in this figure, both O'Rourke and trajectory models predict the spray penetration at various times after the start of injection, suitably. However, the trajectory collision model has presented more exact results, especially at the end of injection procedure during the time interval of (1500:2500µs). However, it can be concluded that the difference between these two collision models has negligible effect on the jet penetration.

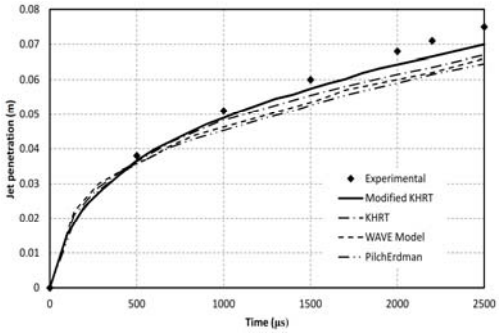

Fig. 7. Comparison of spray jet penetration length for different breakup models (P_{inj}=100MPa).

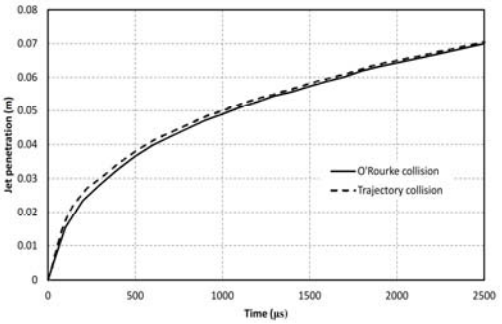

Fig. 8. Comparison of spray jet penetration length for different collision models (P_{inj}=100MPa).

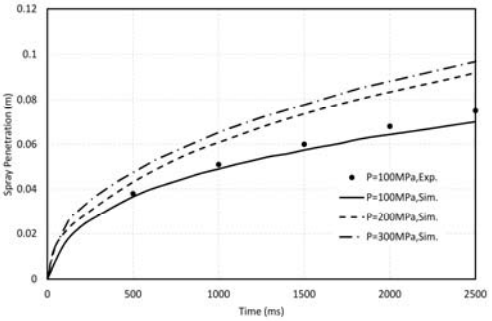

Fig. 9. Effects of injection pressure on spray penetration (Case 1).

Also, the effects of increasing the injection pressure on spray penetration are investigated in Fig. 9. There is a significant increase in spray penetration from 100 to 200 MPa injection pressure. However, this rate of penetration increase is moderate from 200 to 300 MPa. Also, performance of the modified KHRT model has been verified under evaporating condition (Case 2). These results have been presented in Fig. 10. Based on this figure, it is quite evident that the result of vapor penetration of evaporating spray follows the same trend as the non-evaporating results. The RMSE of the spray jet penetration length under evaporating condition is found to be 0.00154.

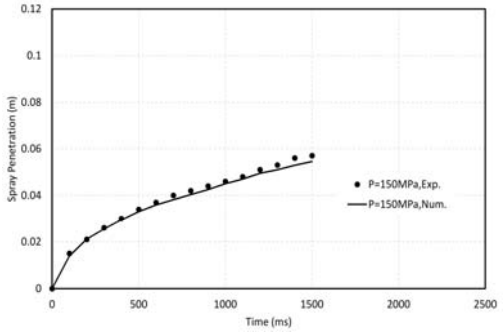

Fig. 10. Comparison of numerical and experimental results of vapor penetration under evaporating condition (Case 2).

Figure 11 presents the variation of spray cone angle at different times after the start of injection. The spray angle is measured based on radial distance at axial location of 40mm. There are some fluctuations in spray angle at various times. Indeed, the difference between KHRT and modified KHRT breakup models on the temporal spray angle is insignificant. Therefore, both of these breakup models can be suggested for determining the spray angle, especially under high injection pressure. This implies that spray angle remains nearly constant during the whole injection time. This phenomenon is in consistent with the finding of other researchers (Turner *et al*., 2012).

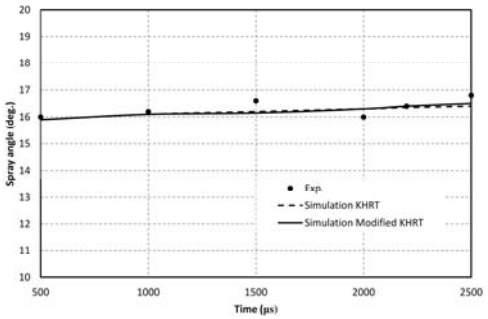

Fig. 11. Spray opening angle vs. time (P_{inj}=100MPa).

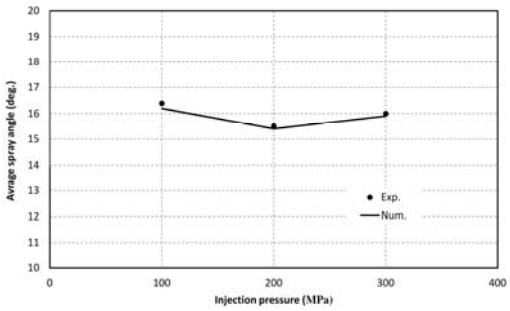

Fig. 12. Mean spray cone angle for different injection pressures (Case 1).

Effects of injection pressure on the mean spray angle are also presented in Fig. 12. It is concluded from Fig. 12 that the injection pressure appears to have little influence (in order of 2% to 4%) on the spray cone angle. In addition, there is no observed change on the average spray angle by an increase or abdecrease in the injection pressure. Based on this figure, one may conclude that the spray angle is not sensitive to the injection pressure. Injection pressure appears to have little influence on the diesel spray angle.

The modified atomization model seems to capture at least some of the important features of spray development. For example, spray penetration and spray angle in transient spray are simulated, more accurately. It is concluded that the advanced KHRT breakup model and trajectory collision model simulate the spray characteristics, more accurately.

4.2 In-Cylinder Gas Motion

Figure 13 shows the gas pressure and velocity contours under P_{inj}=100 MPa. The air velocity vectors change direction toward the spray in the field near the injector. On the other hand, the gas is seen to be pushed out by the spray tip. Between these two main fields, there is a recirculation zone in which velocity vectors have been redirected toward the spray.

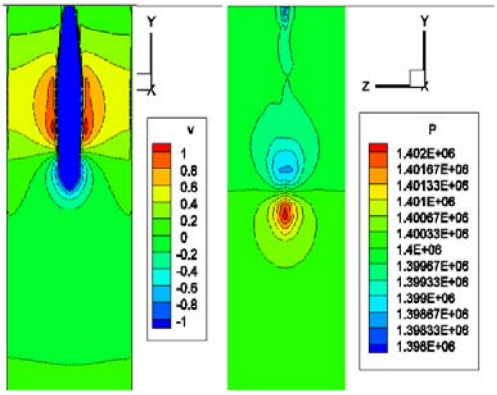

Fig. 13. Gas pressure and axial velocity distribution (P_{inj}=100MPa).

Figure 13 illustrates how a higher-pressure region is formed near the spray tip. In addition, pressure gradient at the outer edge of the spray leads to higher values of velocity in this area.

Sauter Mean Diameter (SMD) is defined as diameter of a sphere that has the same volume/surface area ratio as the entire spray. SMD correlation has been presented by Ejim *et al*. (2007) as follows

$$SMD = 6156\nu^{0.385}\sigma^{0.737}\rho_f^{0.737}\rho_a^{0.06}\Delta P^{-0.54} \quad (18)$$

where ν and σ are the viscosity and surface tension, and ΔP is the pressure difference between injection and ambient pressures. Comparision of the temporal SMD value to the analytical result is presented in Fig.14.

Immediately after the start of injection, high SMD value implies that blob size is equal to the injector diameter. Also, SMD value decreases because of the atomization process of the droplets. Atomization rate increases as the injection time increases.

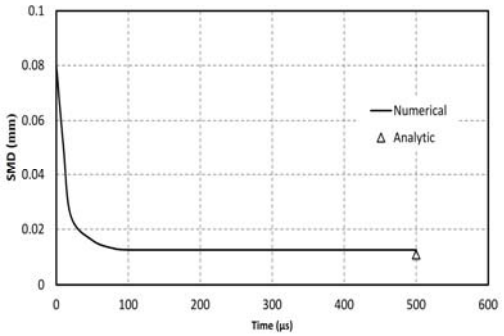

Fig. 14. Comparison of the numerical results of SMD vs. time against analytical value at (P_{inj}=100MPa).

In this case, temporal decrease in SMD from the start of injection until the end of injection is found to be 83.75%.

Droplet diameter can be studied based on Arithmetic Mean diameter (AMD) variation in different positions. AMD values are presented in Fig. 15 for the positions of 20 and 45 mm from the injector. Droplet diameter is observed to increase by increasing the distance from the injector. In addition, by an increase in distance from the injector, temporal decrease in AMD becomes larger.

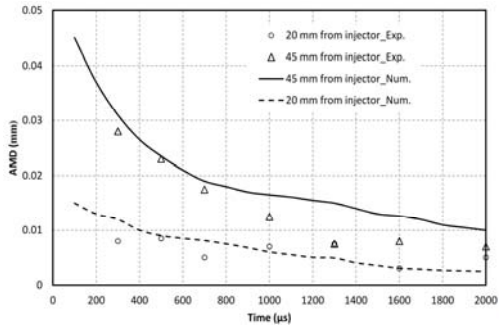

Fig. 15. Temporal variation of AMD in two different positions (P_{inj}=100MPa).

Mixture fraction is an important variable in the spray simulation. Mixture fraction is related to the mass fraction of the fuel stream in the mixture. Radial mixture fraction has been reported in Fig. 16 for two different times after the start of injection at y= 20 mm from the injector. There seems to be an acceptable error in the results of numerical simulation compared with the experimental data at P_{inj}=150 MPa. In Fig. 16 (a), RMSE for the KHRT and modified KHRT breakup models are found to be 0.0181 and 0.0112, respectively. On the other hand, RMSE of the KHRT breakup model in Fig. 16 (b) is equal to be 0.0176, while, for the modified KHRT model, the RMSE is 0.0123. Therefore, it is obvious that the modified KHRT model is more accurate for determining the mixture fraction.

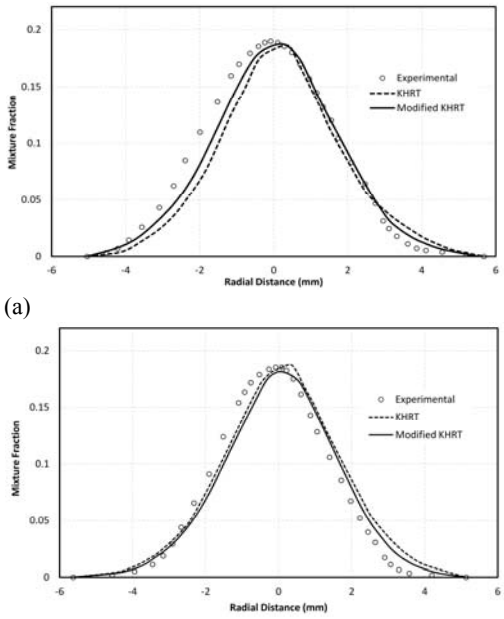

(a)

(b)

Fig. 16. Radial mixture fraction at y= 20 mm from the injector: a) t=0.5 ms, b) t=0.9 ms (Case 3: P_{inj}=150MPa).

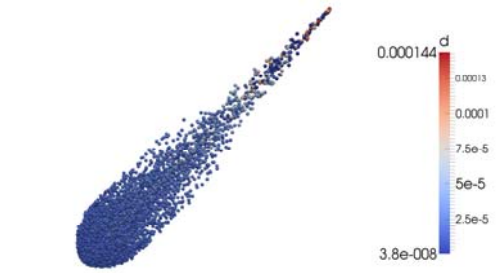

(a): P_{inj}=100MPa, t=1.0ms

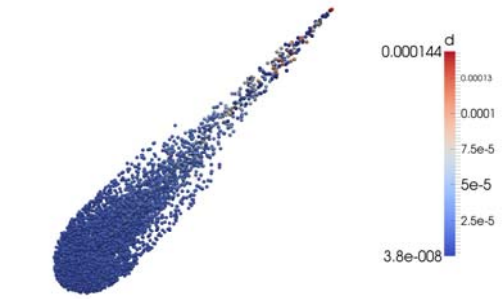

(a): P_{inj}=200MPa, t=1.0ms

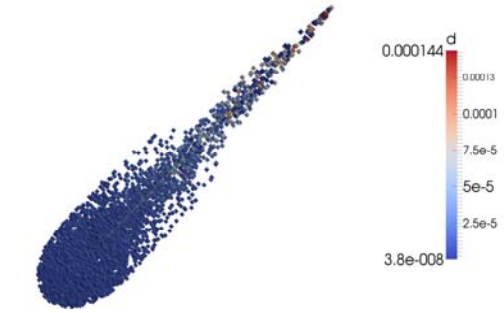

(a): P_{inj}=300MPa, t=1.0ms

Fig. 17. 3-D plot of spray shapes and droplet sizes.

Finally, 3-D plot of spray droplets are shown in Fig. 17. In Fig.17, droplet size is normalized for better presentation of the spray shape. It is quite evident that increasing the injection pressure leads to the reduction of droplet size. Also, larger droplets can be observed in further distances from the injector. These results follow the same trend of Fig. 15.

5. CONCLUSION

Evaporating, non-evaporating and non-reacting ultra-high pressure diesel spray is numerically investigated using various breakup and collision sub-models. Lagrangian particle tracking scheme is implemented for the liquid droplet modeling and RANS method is used to simulate the continuous gas field. Three default breakup models have been employed and a new combined KHRT scheme has been generated. Two different collision models are used and various combinations of sub-models have been compared. Spray penetration length and spray angle at different injection pressures have been compared against the published experimental data for non-evaporating conditions. This comparison has also been carried out using evaporating condition in the field of spray penetration. Good agreement has been achieved between the numerical predictions and measurements reported in the literature for evaporating and non-evaporating conditions.

A new numerically combined breakup model called modified KHRT is also developed for applying the transient effects of injection. Main focus of this study is the evaluation of spray and gas characteristics under ultra-high injection pressures. Based on the obtained results, the new KHRT breakup model predicts jet penetration, spray cone angle, mixture fraction, gas field velocity, and pressure very well at ultra-high pressure injection. Breakup model is proved to have small effect on the jet penetration length and is found to be insignificant. However, effect of the breakup model on the droplet diameter is more obvious. Particularly, in transient spray, the newly proposed model produces more acceptable results. Comparison of the calculated and experimental jet penetration confirms the good performance of the new spray combination model. Results displayed for all of the breakup models indicate that the newly modified sprayFoam solver can be confidently used for simulation of high-pressure diesel injection.

Followings are some of the most important physical observations offered in the current study:

1. Modified KHRT model has presented more accurate spray shape and spray characteristics in wide range of injection pressure.
2. Injection pressure appears to have little influence on the diesel spray angle and spray angle remains nearly constant during the whole injection time.
3. Increasing the injection pressure leads to smaller droplet and yields a decrease in Sauter Mean Diameter (SMD).
4. Numerical results using SprayFoam solver and modified breakup model scheme have shown good agreements with the experimental results for both the spray characteristics and induced gas motion and pressure.

Finally, poor mixing and entrainment lead to larger liquid fuel fraction. Accordingly, higher liquid volume fractions are observed near the spray axis, where the poor mixing occurs.

REFERENCES

Baumgarten, C. (2006). Mixture Formation in Internal Combustion Engine. Springer Science and Business Media, New Delhi, India.

Ejim, C. M., B. A. Fleck and A. Amirfazli (2007). Analytical study for atomization of biodiesels and their blends in a typical injector: surface tension and viscosity effects. *Fuel* 86, 1534–1544.

Erdman, C. A. and M. Pilch (1987). Use of breakup time data and velocity history data to predict the maximum size of stable fragments for acceleration-induced breakup of a liquid drop. *International Journal of Multiphase Flow* 13(6), 741–757.

Ferziger, J. H. and M. Peric (2002). Computational methods for fluid dynamics. Springer-Verlag Berlin Heidelberg, New York, USA.

Ghadimi, P. and H. Nowruzi (2016). Effects of heavy fuel oil blend with ethanol, n-butanol or methanol bioalcohols on the spray characteristics. Journal of Applied Fluid Mechanics, 9(5), 2413-2425.

Gjesing, R., J. Hattel and U. Fritsching (2009) Coupled atomization and spray modelling in the spray forming process using OpenFOAM. Engineering *Applications of Computational Fluid Mechanics* 3(4), 471-486.

Heywood, J. B. (1988). *Internal Combustion Engine Fundamentals*, McGraw-Hill.

Hosseinpour, S. and A. R. Binesh (2009). Investigation of fuel spray atomization in a DI heavy-duty diesel engine and comparison of various spray breakup model. Fuel, 88, 799-805.

Jones, W. P. and B. E. Launder (1972). The prediction of laminarization with a two-equation model of turbulence. *International Journal of Heat and Mass Transfer* 15, 301–314.

Kamali, R. and M. Mofarrahi (2012). Numerical investigation of various spray breakup and droplet collision models in the modeling of in-cylinder fuel spray. *Atomization and Sprays* 22(10), 843–860.

Kassem, H. I., K. M. Saqr, H. S. Aly and *et al*. (2011). Implementation of the eddy dissipation model of turbulent non-premixed combustion in OpenFOAM. *International Communications*

in Heat and Mass Transfer 38, 363-367.

Moreira, A. L. N., A. S. Moita and M. R. Panao (2010). Advances and challenges explaining fuel spray impingement: How much of single droplet impact research is useful?. *Progress in Energy Combustion Science* 36, 54-580.

Nordin, N. (2001). *Complex Chemistry Modeling Of Diesel Spray Combustion*. Ph. D. thesis, Dept. of Thermo and Fluid Dynamics, Chalmers University of Technology, Goteborg, Sweden.

O'Rourke, P. J. and F. V. Bracco (1980). Modelling of drop interactions in thick sprays and a comparison with experiments. *Proc I Mech E* 9, 101–116.

O'Rourke, P. J. and A. A. Amsden (1987) The TAB Method for Numerical Calculation of Spray Droplet Breakup. *SAE International Fuels and Lubricants Meeting and Exposition, Toronto, Ontario 872089.*

Pei, Y., M.J. Davis, L.M. Pickett and S. Som (2015). Engine Combustion Network (ECN): Global sensitivity analysis of Spray A for different combustion vessels. Combustion and Flame, 162(6), 2337-2347.

Reitz, R. D. (1987). Modeling atomization processes in high-pressure vaporizing sprays. *Atomization and Spray Technology* 3, 309-337.

Reitz, R. D. and F. V. Bracco (1982). Mechanism of atomization of a liquid jet. *Phys. Fluids* 25, 1730-1741.

Reitz, R. D. and R. Diwakar (1987). Structure of high-pressure fuel sprays. *SAE; Technical Paper* 870598.

Roisman, I. V., L. Araneo and C. Tropea (2007). Effect of ambient pressure on penetration of a diesel spray. *Int. J. Multiphase Flow* 33, 904-920.

Sazhin, S. S., S. B. Martynov, T. Kristyadi and *et al*. (2008). Diesel fuel spray penetration, heating, evaporation and ignition: modeling versus experimentation. *Int. J. Engineering Systems and Modelling* 1(1), 1-19.

Shervani-Tabar, M. T., M. Sheykhvazayefi and M. Ghorbani (2013). Numerical study on the effect of the injection pressure on spray penetration length. *Applied Mathematical Modelling* 37, 7778-7788.

Som, S. and S. K. Aggarwal (2010). Effects of primary breakup modeling on spray and combustion characteristics of compression ignition engines. *Combust. Flame* 157, 1179-1193.

Stiesch, G. (2003). Modeling Engine Spray and Combustion Processes. Springer Science & Business Media, New York, USA.

Tanner, F. X. (1997). Liquid jet atomization and droplet breakup modeling of non-evaporating diesel fuel sprays. *SAE, Technical Paper* 970050.

Taylor, G. (1950). The instability of liquid surface when accelerated in a direction perpendicular to their planes. *Proceedings of the Royal Society of London* 201, 192-196.

Turner, M. R., S. S. Sazhin, J. J. Healey and *et al*. (2012). A breakup model for transient diesel fuel sprays. *Fuel* 97, 288-305.

Vuorinen, V., C. Duwig, L. Fuchs and *et al*. (2011). large-eddy simulation of a compressible spray using eulerian-eulerian approach. *In 24th European Conference on Liquid Atomization and Spray Systems*, Estoril, Portugal.

Wang, X., Z. Huang, O. A. Kuti and *et al*. (2010). Experimental and analytical study on biodiesel and diesel spray characteristics under ultra-high injection pressure. *Int. J. Heat Fluid Flow* 31, 659–666.

Wehrfritz, A., V. Vuorinen, O. Kaario and M. Larmi (2013). Large Eddy Simulation of high-velocity fuel sprays: studying mesh resolution and breakup model effects for spray A. *Atomization and Sprays* 23(5), 419–442.

Xue, Q., M. Battistoni, S. Som and *et al*. (2014). Eulerian CFD modeling of coupled nozzle flow and spray with validation against x-ray radiography data. *SAE* 2014-01-1425.

Yousefifard, M., P. Ghadimi and H. Nowruzi (2015). Numerical investigation of the effects of chamber backpressure on HFO spray characteristics. *International Journal of Automotive Technology* 16(2), 339-349.

Yousefifard, M., P. Ghadimi and H. Nowruzi, (2014). Three-dimensional LES modeling of induced gas motion under the influence of injection pressure and ambient density in an ultrahigh-pressure diesel injector. Journal of the Brazilian Society of Mechanical Sciences and Engineering, 37(4), 1235-1243.

Yousefifard, M., P. Ghadimi and M. Mirsalim (2014). Numerical simulation of biodiesel spray under ultra-high injection pressure using OpenFOAM. Journal of the Brazilian Society of Mechanical Sciences and Engineering, 37(2), 737-746.

Zhu, J., K. Nishida and T. Uemura (2014). Experimental study on flow fields of fuel droplets and ambient gas of diesel spray-free spray and flat-wall impinging spray. *Atomization and Sprays* 24(7), 599–623.

Zhu, J., O. A. Kuti and K. Nishida (2012). An investigation of the effects of fuel injection pressure, ambient gas density and nozzle hole diameter on surrounding gas flow of a single diesel spray by the laser-induced fluorescence particle image velocimetry technique. International J of Engine Research, 14(6), 630-645.